Article published online: 2023-08-21

The Role of Multimodal Imaging in Differentiating Vasogenic from Infiltrative Edema: A Systematic Review

Alireza Hasanzadeh[1,2,*] Hossein Sanjari Moghaddam[1,2,*] Madjid Shakiba[2] Amir Hossein Jalali[2] Kavous Firouznia[2]

[1] Medical School, Tehran University of Medical Sciences, Tehran, Iran
[2] Advanced Diagnostic and Interventional Radiology Research Center, Tehran University of Medical Sciences, Tehran, Iran

Address for correspondence Kavous Firouznia, MD, Medical Imaging Center, Imam Khomeini Hospital, Tehran University of Medical Sciences, Tehran, Iran (e-mail: k_firouznia@yahoo.com).

Indian J Radiol Imaging 2023;33:514–521.

Abstract

Background High-grade gliomas (HGGs) are the most prevalent primary malignancy of the central nervous system. The tumor results in vasogenic and infiltrative edema . Exact anatomical differentiation of these edemas is so important for surgical planning. Multimodal imaging could be used to differentiate the edema type.

Purpose The aim of this study was to investigate the role of multimodal imaging in the differentiation of vasogenic edema from infiltrative edema in patients with HGG (grade III and grade IV).

Data Sources A search on PubMed, EMBASE, Scopus, and ISI Web of Science Core Collection up to June 2022 using terms related to (a) multimodal imaging AND (b) HGG AND (c) edema. (PROSPERO registration number: CRD42022336131)

Study Selection Two reviewers screened the articles and independently extracted the data. We included original articles assessing the role of multimodal imaging in differentiating vasogenic from infiltrative edema in patients with HGG. Six high-quality articles remained for the narrative synthesis.

Data Synthesis Dynamic susceptibility contrast imaging showed that relative cerebral blood volume and relative cerebral blood flow were higher in the infiltrative edema component than in the vasogenic edema component. Diffusion tensor imaging revealed a dispute on fractional anisotropy. The apparent diffusion coefficient was comparable between the two edematous components. Magnetic resonance spectroscopy exhibited an increment in choline/creatinine ratio and choline/N-acetyl aspartate ratio in the infiltrative edema component.

Limitations Strict study selection, low sample size of relevant published studies, and heterogeneity in endpoint variables were the major drawbacks.

Conclusions Multimodal imaging, including dynamic susceptibility contrast and magnetic resonance spectroscopy, might help differentiate between vasogenic and infiltrative edema.

Keywords
- glioma
- infiltrative edema
- systematic review
- vasogenic edema

* *A.H and H.S.M contributed equally to this study.*

article published online
August 21, 2023

DOI https://doi.org/10.1055/s-0043-1772466.
ISSN 0971-3026.

Thieme Medical and Scientific Publishers Pvt. Ltd., A-12, 2nd Floor, Sector 2, Noida-201301 UP, India

Introduction

High-grade gliomas (HGGs) are the most prevalent primary malignancy of central nervous system. HGGs include World Health Organization (WHO) grade III and IV.[1] HGGs have a yearly incidence of 3.68 per 100,000.[2,3] Grade III HGGs are associated with a median survival of 14 to 36 months, whereas grade IV HGGs are associated with a median survival of only 9 to 15 months.[4,5]

Although brain tumors have diverse morphologic and biological properties, they are associated with disruption of the blood–brain barrier and thus the development of cerebral edema.[6,7] Edema related to brain tumors can be categorized into two main types: vasogenic and infiltrative edema. The most common form of edema in brain tumors is vasogenic edema.[8] In vasogenic edema, the blood–brain barrier is locally disrupted leading to elevated capillary permeability and induction of a pressure gradient from the vascular to the extracellular compartment. This chain of events leads to the retention of plasma fluid and protein in the extracellular space.[9] Second type of edema is infiltrating that means edema associated with tumoral cells that are target of surgical excision. Neurosurgical operation plans are chosen very precise as the neurosurgical excisions should be done exactly as necessary as possible with no unnecessary damage to healthy tissues.

Differentiation of these two types of edema is so important as the infiltrating edema in contrast to vasogenic edema should be diagnosed before surgical plan in order to be excised as accurate as possible during surgery. T2 prolongation indicates both vasogenic edema and infiltrating tumor cells outside of contrast-enhancing lesions in primary HGGs.[10,11] This is while vasogenic edema comprises T2 prolongation surrounding meningiomas and brain metastases.[8]

Various conventional (T1- and T2-weighted sequences) and advanced magnetic resonance imaging (MRI) modalities such as perfusion-weighted imaging (PWI), diffusion-weighted imaging (DWI), and MR spectroscopy (MRS),[12,13] positron emission tomography (PET)/computed tomography (PET/CT)[14] can be used to investigate tumor structure and heterogeneity. These advanced techniques use different approaches to identify tissue composition. PWI measures the tissue microvasculature and indicates the neoangiogenesis and malignancy of the tumor. PWI produces indices, including cerebral blood volume (CBV), mean transit time, cerebral blood flow (CBF), and percentage of signal intensity recovery (PSR). The most reliable and most extensively-used measure of tumor microvasculature is relative CBV (rCBV).[15–17] DWI produces a measure called apparent diffusion coefficient (ADC), which measures the diffusion of water molecules in biological tissues. ADC is generally negatively associated with glioma grade.[18,19] MRS indicates the histological grade of the tumor by measuring metabolites, such as choline (Cho), creatine (Cr), N-acetylaspartate (NAA), myo-inositol (MI), lipids and lactate (LL). For instance, tumor grade and malignancy are correlated with an increase of Cho with a reduction of NAA and resulting deviations of Cho/Cr and NAA/Cho ratios.[17] Finally, PET imaging with 2-[18F]-fluoro-2-deoxy-D-glucose (18F-FDG) has valuable application in brain tumors.[20] 18F-FDG uptake, which can be measured by the maximum standardized uptake value (SUVmax) or the local metabolic rate of glucose, is increased in high-grade tumors.[21] These imaging modalities can be useful in the differentiation of vasogenic from infiltrative edema surrounding the glioma tumors. In this systematic review, we aimed to investigate the role of different imaging modalities in the differentiation of vasogenic from infiltrative edema in HGGs.

Methods

Information Sources and Search Strategy

This study was performed in concordance with the Preferred Reporting Items for Systematic Review and Meta-Analysis (PRISMA) 2020 statement. The protocol of this review was registered in the PROSPERO database (registration number: CRD42022336131) before the search began. We performed a search on PubMed, EMBASE, Scopus, and ISI Web of Science Core Collection by using keywords chosen based on the MeSH thesaurus without language or date restriction on June 1, 2022. Included studies were original publications that studied the role of multimodal imaging in delineating infiltrative edema from vasogenic edema in patients with HGG. Therefore, the terms searched were related to multimodal imaging AND HGG AND edema.

Search Strategy

We included original articles assessing the role of multimodal imaging in differentiating vasogenic from infiltrative edema in patients with HGG (grade III and grade IV). PubMed search terms are presented as follows:

(a) ((((((((((((((((((((((((multimodal imaging[MeSH]) OR (magnetic resonance imaging[Title/abstract])) OR (mri[Title/abstract])) OR (functional mri[Title/abstract])) OR (fmri[Title/abstract])) OR (functional magnetic resonance imaging[Title/abstract])) OR (magnetic resonance spectroscopy[Title/abstract])) OR (mrs [Title/abstract])) OR (spectroscopy[Title/abstract])) OR (positron emission tomography[Title/abstract])) OR (pet[Title/abstract])) OR (spect[Title/abstract])) OR (single photon emission computed tomography[-Title/abstract])) OR (dti[Title/abstract])) OR (diffusion tensor imaging[Title/abstract])) OR (bold[Title/abstract])) OR (blood oxygen level dependent[Title/abstract])) OR (pwi[Title/abstract])) OR (perfusion-weighted imaging[Title/abstract])) OR (diffusion-weighted imaging[Title/abstract])) OR (pet ct[Title/abstract])) OR (dwi[Title/abstract])) OR (t1[Title/abstract])) OR (t2[Title/abstract]))

(b) (((((((glioma[Title/abstract]) OR (high-grade glioma [Title/abstract])) OR (malignant glioma[-Title/abstract])) OR (glioblastoma[Title/abstract])) OR (astrocytoma[Title/abstract])) OR (oligodendroglioma[Title/abstract]))

(c)(edema[Title/abstract])

The final search in all databases was as follows: (a) AND (b) AND (c).

Two reviewers screened the titles and abstracts independently. Any disagreements were discussed and resolved by the third reviewer if required. Duplicate articles, nonhuman studies, letters, and reviews were excluded.

Data Extraction

EndNote 20 was used to remove duplicate citations and the screening, and predefined Microsoft Word 2016 was used to record variables extracted from the included articles. Two authors independently extracted the data. Any disagreement was resolved through consultation with the senior author. The following variables were collected from studies: design of each study, number of patients, participating, age of patients, female to male ratio, confirmation, imaging techniques, metrics of each study, and their results.

Risk of Bias

The Joanna Briggs Institute (JBI) Critical Appraisal Checklist for the analytical cross-sectional study was used to assess the possible risk of bias among the included studies.[22]

Results

A PRISMA flow diagram outlining our search results at each step can be found in ►**Fig. 1**. Initial records identified through our literature search yielded 3625 articles. In total, 1685 articles were excluded because they were duplicates. We excluded nonoriginal, nonhuman, or unavailable full texts. One hundred sixteen full texts were assessed for eligibility. After excluding 110 articles that did not meet the inclusion criteria (such as including low-grade glioma, including metastases or meningioma, and not comparing vasogenic from infiltrative edema), only six studies remained for the qualitative analysis. ►**Table 1** shows the main characteristics and outcome data of the included

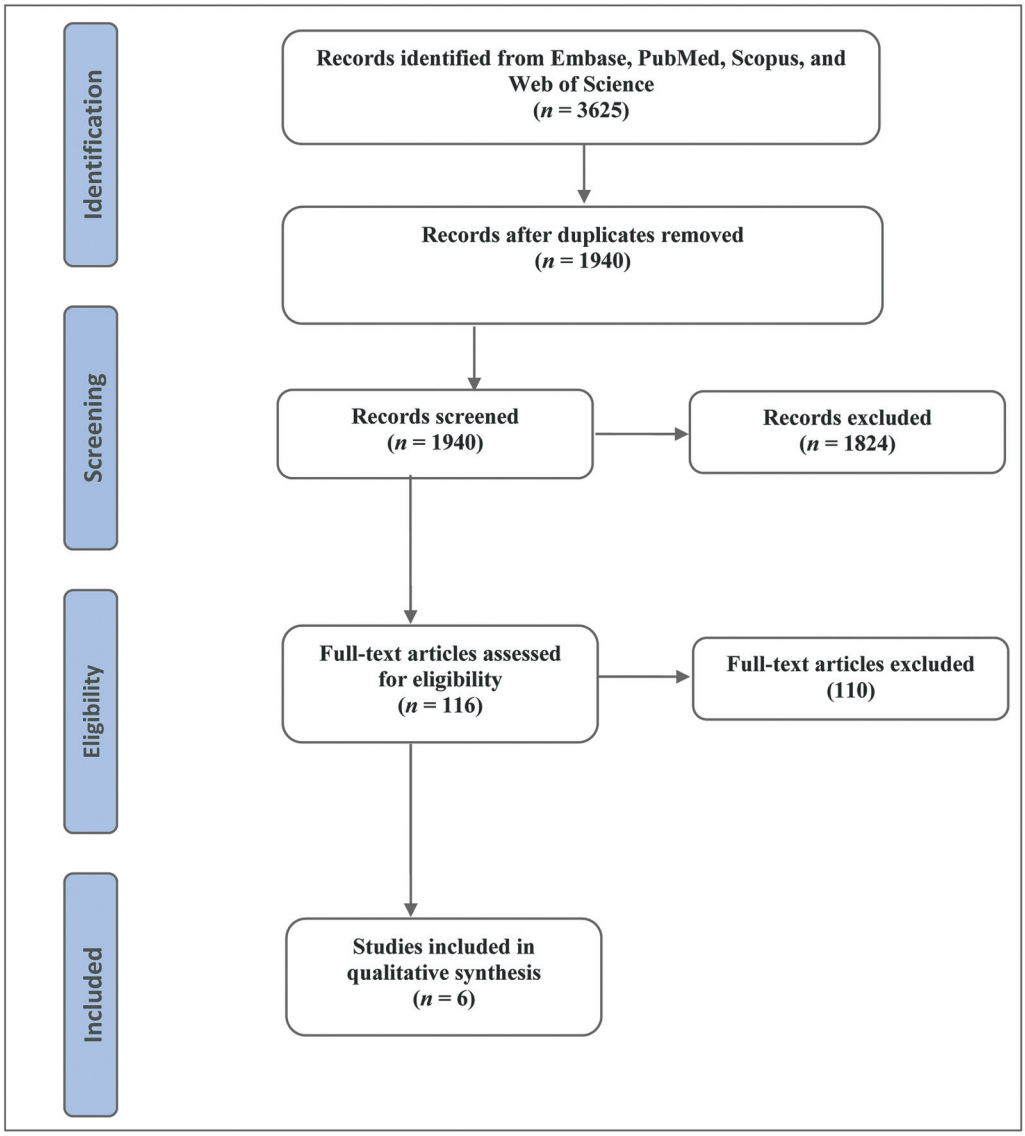

Fig. 1 Preferred Reporting Items for Systematic Review and Meta-Analysis (PRISMA) flow diagram.

Table 1 Characteristics of the included studies

First author, Year	*n*, Male, MA, grade	Imaging techniques	Confirmation	Metrics and results
Oh et al, 2005[27]	16, NR, NR, (III:2, IV: 14)	DTI, T_2WI	Radiological segmentation: Immediate-edema: Non-enhancing T2 anomaly within 1-cm margin. Peripheral edema: Non-enhancing T2 anomaly outside the 1-cm margin	The ADC values in the immediate-edema (1436 ± 241) and peripheral-edema (1573 ± 302) regions were significantly higher than those in the tumor (1279 ± 206). No significant differences in ADC values were noted between the immediate- and peripheral-edema regions. The T2 relaxation values in both the immediate- edema (204 ± 33) and peripheral edema (220 ± 42) regions were significantly higher than those of the tumor (160 ± 31). The T2 relaxation values in the immediate- and peripheral-edema regions were not significantly different. The ADC and T2 values correlated significantly (r: 0.95) The ADC and T2 relaxation values in the immediate- and peripheral-edema regions were significantly higher than the NAWM
Artzi et al, 2014[23]	14, 8, 52, IV	T1WI/T1WI + Gad, T2WI, FLAIR, DSC, DCE, DTI, MRS	Unsupervised multiparametric classification based on statistical optimization MRS was used for validation of the classification	Vasogenic edema had lower rCBV (0.71 ± 0.20), rCBF (0.66 ± 0.20), EnT_1WI (3.43 ± 3.14), MD (1.29 ± 0.26), k^{trans} (0.59 ± 1.09), V_p (1.58 ± 1.76), Cho/Cr ratio (1.25 ± 0.27) and increased rFLAIR (1.41 ± 0.13) compared to infiltrative edema (1.68 ± 0.51, 1.64 ± 0.50, 5.22 ± 3.77, 1.20 ± 0.25, 0.84 ± 1.39, 1.63 ± 0.27, 2.48 ± 3.14; respectively) Infiltrative edema had increased rCBV, rCBF, and EnT_1WI compared to NAWM
Artzi et al, 2015[26]	19, 7, 53, IV	T1WI/T1WI + Gad, FLAIR, DSC, DCE, MRS	Unsupervised multiparametric classification based on statistical optimization MRS was used for validation of the classification	Infiltrative edema had higher rCBV (1.80 ± 0.43), rCBF (1.34 ± 0.32) and Cho/Cr ratio (1.51 ± 0.13) than Vasogenic edema (0.68 ± 0.16, 0.62 ± 0.18 and 1.19 ± 0.09, respectively) Vasogenic edema had the lowest rCBV and rCBF.
Valentini et al, 2017[25]	12, 7, 65, IV	T1WI/T1WI + Gad, T2WI, and FLAIR, DTI, MRS, 18F-FDG PET/CT	Histological analysis Radiological segmentation: Immediate-edema: Non-enhancing T2 anomaly within 1-cm margin. Peripheral edema: Non-enhancing T2 anomaly outside the 1-cm margin	Infiltrative edema had higher rCBV (2.42 (0.89-4.39)), Cho/Cr ratio (1.86 (0.97-2.24)), and Cho/NAA ratio (1.83 (0.75-4.04)) and lower FA values (0.29 (0.10-0.33)) than vasogenic edema (1.23 (0.60-2.40), 1.47 (0.96-2.99), 1.08 (0.74-1.85), and 0.28 (0.10-0.47), respectively). rT2 FSE and rT2 FLAIR were not specific for edematous areas
Molina-Romero et al, 2018[28]	25, NR, NR, IV	DTI	Radiological segmentation	Both infiltration and edema had decreased FA compared to NAWM. Vasogenic edema had lower FA compared to tumor infiltration
Wu et al, 2019	44, 27, 64, (III:19, IV: 25)	T1WI/T1WI + Gad, T2WI, FLAIR, DSC-PWI	Radiological segmentation	Vasogenic edema had lower rCBV and rCBF compared to infiltrative edema and other tumor parts

Abbreviations: 18F-FDG PET/CT, 18-fluorine-fluorodeoxyglucose positron emission tomography/computed tomography; ADC, apparent diffusion coefficient; Cho/Cr, Choline/Creatine; Cho/NAA, Choline/N-acetyl aspartate; DCE, dynamic contrast enhancement imaging; DSC, diffusion and dynamic susceptibility contrast imaging; DTI, diffusion tensor imaging; EnT_1WI, T1WI enhancement; FA, fractional anisotropy; FLAIR, fluid attenuated inversion recovery; FSE, fast spin echo; Gad, gadolinium; k^{trans}, vascular permeability; MA, mean age; MD, mean diffusivity; MRS, magnetic resonance spectroscopy; N, number; NAWM, normal appearing white matter; NR, not reported; PWI, perfusion weighted imaging; rCBF, relative cerebral blood flow; rCBV, relative cerebral blood volume; rFLAIR, relative fluid attenuated inversion recovery; T_1WI, T1 weighted imaging; T_2WI, T2 weighted imaging; V_p, plasma volume.

studies. Given the heterogeneity among the studies, meta-analysis was not possible.

From a total of 130 patients included in this review, only 21 patients had grade III glioma, and the other 109 subjects had grade IV glioma. Original articles were from Israel, China, Italy, Germany, and the United States, and all of them were conducted in a prospective manner.

The JBI Critical Appraisal Checklist for analytical cross-sectional study showed that all of the six included studies have a low risk of bias and could be used in data synthesis.

Relative Cerebral Blood Volume and Relative Cerebral Blood Flow

Dynamic susceptibility contrast magnetic resonance imaging (DSC) was performed in four original articles. All these three studies showed that relative cerebral blood volume (rCBV) was higher in the infiltrative edema component than in the vasogenic edema component [0.71 (0.20) vs. 1.68 (0.51), 1.80 (0.43) vs. 1.19 (0.09), and 2.42 (interquartile range: 0.89–4.39) vs. 1.23 (0.60–2.40)].[23–26] Similarly, two of the studies revealed that relative cerebral blood flow (rCBF) was higher in infiltrative edema than in vasogenic edema [0.66 (0.20) vs. 1.64 (0.50), 1.34 (0.32) vs. 0.62 (0.18)].[23,24]

Fractional Anisotropy and Apparent Diffusion Coefficient

Four of the studies implemented diffusion tensor imaging (DTI) to assess edema.[23,25,27,28] Fractional anisotropy (FA) was reported to be lower in the vasogenic edema component than in the infiltrative edema component in the study performed by Molina-Romero et al. However, Valentini et al reached the opposite results [0.29 (0.10-0.33) vs. 0.28 (0.10-0.47)] . On the other hand, the ADC was not significantly different between the two edematous components.

Choline/Creatinine Ratio

MRS was done in the studies by Artzi et al and Valentini et al.[23,25,26] They found that the Cho/Cr was higher in the infiltrative edema component than in the vasogenic edema parts [1.51 (0.13) vs. 1.19 (0.09), 1.86 (0.97–2.24) vs. 1.08 (0.74–1.85)]. Valentini et al also showed that Cho/NAA was higher in the infiltrative edema component [1.83 (0.75–4.04) vs. 0.28 (0.10–0.47)].

Discussion

The failure of local control of the tumor is a consequence of the invasion capacity of tumor cells since infiltrating tumor cells can spread far from the tumor and thus escape radiation effects. Infiltrating tumor cells are detected in peritumor edema[29] and in normally-appearing regions in 20% of glioblastoma.[30] MRI is unable to detect these infiltrative cells when occurring in T2 hyperintense or normal T1 or T2 regions. It is vital to recognize tumor infiltration in edematous regions.[31] Edematous regions of MRI are histologically characterized by a higher expression of Aquaporin 4.[32] The detection of infiltrative tumor cells in these areas depends on their frequency. Edema might confound the MRI variables and the total cell number (regardless of the nature of the cells), and thus, it is harder to identify tumor infiltration when it overlaps with edema.[33,34] In edematous situations, cell density (both normal and tumor cells) is reduced and thus tumor infiltration is identifiable when cell density is higher than normal so that it can influence MRI variables.[35]

Conventionally, it is believed that surrounding edema around tumors like meningioma and brain metastasis are purely vasogenic and the surrounding edema around HGG is infiltrative in nature. However, in the past years, several studies have demonstrated that edema associated with HGG has both vasogenic and infiltrative components. The subsequent studies have tried to use different imaging modalities to differentiate vasogenic and infiltrative components of edema around HGG. This is the first study to systematically review the current imaging evidence for the differentiation of infiltrative and vasogenic edema surrounding grade III to IV glioma. We hypothesized that infiltrative and vasogenic edema have distinct features of different imaging modalities so that they can be correctly differentiated leading to better treatment strategies in patients with HGG.

Our findings showed that most imaging modalities are able to produce measures to differentiate between vasogenic and infiltrative edema. The results from perfusion studies showed that vasogenic edema had lower rCBV[23–26] and rCBF[23,24] compared to infiltrative edema. rCBV, PH, and PSR are the main perfusion parameters that correlate with tumor microvasculature.[15,16,36] Moreover, rCBV variations are a reliable indicator of the microvasculature and histological grade of the tumor.[37–39] In Valentini et al's study,[25] rCBV values reduce from contrast-enhancing to noncontrast-enhancing regions with higher values in infiltrated areas with microvascular proliferation indicating neoangiogenesis.

Regarding the MRS studies, it was shown that Cho/Cr and Cho/NAA ratio values were higher in infiltrative compared to vasogenic edema.[23,25,26] Based on previous evidence, a high Cho/NAA ratio in edematous areas is indicative of tumor infiltration.[40–42] However, lower absolute values of total NAA appear to be more reliable than Cho to suggest low tumor infiltration.[43] In Valentini et al's study,[25] 18F-FDG SUVmax, Cho/Cr, and Cho/NAA ratio were the most accurate measure of tumor infiltration in edematous regions.

The results of diffusion studies were inconsistent. One study showed that FA values were lower in edematous areas with infiltration than without infiltration.[25] This is while another study demonstrated that tumor edema had lower FA compared to tumor infiltration.[44] Moreover, another study reported that vasogenic edema had lower MD compared to infiltrative edema.[23] Decreased levels of FA values are found in both CE and NE regions compared to normal brain. Interestingly, this reduction in FA is bolder in infiltrated regions compared to the CE region without necrosis or to infiltrated regions with microvascular proliferations, where the presence of microstructural barriers related to the high cell density and vascular proliferations leads to relatively higher FA values.[45,46] Glioblastoma tends to spread along white matter tracts leading to white matter disintegration that can be detected by DTI. Nonetheless, infiltration regions

with or without microvascular proliferation and with edema have shown no significant differences in FA measurements, which are in agreement with previous evidence suggesting a low sensitivity of FA decrease for detection of infiltration.[47–49]

Moreover, one of the review studies reported that ADC is not able to differentiate between infiltrative and vasogenic edema.[27] In fact, no association has been observed between ADC values and the tumor histopathological findings. Generally, tumor parenchyma ADC is an indirect index of cell proliferation and malignancy,[50,51] and should be inversely associated with tumor grade (i.e., lower ADC values in hypercellular areas).[18,19,52] There is an inverse correlation between 18F-FDGSUVmax and ADCmin, and between SUV ratio and ADCmin[53]; however, ADC is not an appropriate measure for tumor grade identification.[54,55] Valentini et al[25] found a similar ADC profile in CE and NE regions, but a lower ADC value in edema, where water is copious. ADC measurements can be affected by several factors. For instance, necrosis-related enlargement of the extracellular compartment might reveal the effect of high cellularity. Instead, nontumor reactive cells such as astrocytes and microglia/macrophages might be present in edematous areas leading to reduced ADC.

This systematic review is not without limitations. The main limitation is the low number of studies that have studied the differentiation of infiltrative and vasogenic edema in HGG. This might be due to our strict inclusion and exclusion criteria since we did not include other types of brain tumors or even low-grade gliomas. The other limitation is the heterogeneity of modalities for the differentiation of infiltrative and vasogenic edema. This prevents the implementation of meta-analysis and production of quantitative results. The other limitation was the diverse definition of infiltrative and vasogenic edema across studies, which might confound the conclusion of this study. We suggest conducting further studies assessing these modalities to reach a comprehensible result. Besides, it is worth evaluating other parameters including peak height and percentage of signal recovery.[56]

Conclusion

In conclusion, it has been shown that edema associated with HGG has both vasogenic and infiltrative components and several studies have been implemented to differentiate between these two. The subsequent studies have tried to use different imaging modalities to differentiate vasogenic and infiltrative components of edema around HGG. In this systematic review, the current imaging evidence for the differentiation of infiltrative and vasogenic edema surrounding grade III to IV glioma was investigated. Our findings demonstrated that multimodal imaging, including DSC, and MRS might be helpful to differentiate between vasogenic and infiltrative edema.

Author Contributions

AH was involved in data curation, investigation, drafting, and revision; HSM helped in data curation, investigation, drafting, and revision; MSh contributed to data curation, investigation, supervision, and revision; AHJ helped in conceptualization, methodology, and supervision; KF contributed to conceptualization, supervision, project administration, and revision. All authors read and approved the final manuscript.

Data Availability Statement

This article is a systematic review using previously published articles.

Funding

None.

Conflicts of Interest

None declared.

References

1 de Groot JF. High-grade gliomas. Continuum (Minneap Minn) 2015;21(2 Neuro-oncology):332–344
2 Ostrom QT, Gittleman H, Liao P, et al. CBTRUS Statistical Report: Primary brain and other central nervous system tumors diagnosed in the United States in 2010-2014. Neuro-oncol 2017;19 (suppl_5):v1–v88
3 Ostrom QT, Gittleman H, Stetson L, Virk SM, Barnholtz-Sloan JS. Epidemiology of gliomas. Cancer Treat Res 2015;163:1–14
4 Linkous AG, Yazlovitskaya EM. Angiogenesis in glioblastoma multiforme: navigating the maze. Anticancer Agents Med Chem 2011;11(08):712–718
5 De Bonis P, Lofrese G, Anile C, Pompucci A, Vigo V, Mangiola A. Radioimmunotherapy for high-grade glioma. Immunotherapy 2013;5(06):647–659
6 Klatzo I. Pathophysiological aspects of brain edema. Acta Neuropathol 1987;72(03):236–239
7 Kuroiwa T, Cahn R, Juhler M, Goping G, Campbell G, Klatzo I. Role of extracellular proteins in the dynamics of vasogenic brain edema. Acta Neuropathol 1985;66(01):3–11
8 Strugar J, Rothbart D, Harrington W, Criscuolo GR. Vascular permeability factor in brain metastases: correlation with vasogenic brain edema and tumor angiogenesis. J Neurosurg 1994;81 (04):560–566
9 Reulen HJ, Graham R, Spatz M, Klatzo I. Role of pressure gradients and bulk flow in dynamics of vasogenic brain edema. J Neurosurg 1977;46(01):24–35
10 Kelly PJ, Daumas-Duport C, Scheithauer BW, Kall BA, Kispert DB. Stereotactic histologic correlations of computed tomography- and magnetic resonance imaging-defined abnormalities in patients with glial neoplasms. Mayo Clin Proc 1987;62(06): 450–459
11 Bertossi M, Virgintino D, Maiorano E, Occhiogrosso M, Roncali L. Ultrastructural and morphometric investigation of human brain capillaries in normal and peritumoral tissues. Ultrastruct Pathol 1997;21(01):41–49
12 Stadlbauer A, Prante O, Nimsky C, et al. Metabolic imaging of cerebral gliomas: spatial correlation of changes in O-(2-18F-fluoroethyl)-L-tyrosine PET and proton magnetic resonance spectroscopic imaging. J Nucl Med 2008;49(05):721–729
13 Di Costanzo A, Scarabino T, Trojsi F, et al. Proton MR spectroscopy of cerebral gliomas at 3 T: spatial heterogeneity, and tumour grade and extent. Eur Radiol 2008;18(08):1727–1735
14 Chen W. Clinical applications of PET in brain tumors. J Nucl Med 2007;48(09):1468–1481
15 Barajas RF Jr, Hodgson JG, Chang JS, et al. Glioblastoma multiforme regional genetic and cellular expression patterns: influence

on anatomic and physiologic MR imaging. Radiology 2010;254 (02):564–576
16 Barajas RF Jr, Phillips JJ, Parvataneni R, et al. Regional variation in histopathologic features of tumor specimens from treatment-naive glioblastoma correlates with anatomic and physiologic MR Imaging. Neuro-oncol 2012;14(07):942–954
17 Fudaba H, Shimomura T, Abe T, et al. Comparison of multiple parameters obtained on 3T pulsed arterial spin-labeling, diffusion tensor imaging, and MRS and the Ki-67 labeling index in evaluating glioma grading. Am J Neuroradiol 2014;35(11):2091–2098
18 Kitis O, Altay H, Calli C, Yunten N, Akalin T, Yurtseven T. Minimum apparent diffusion coefficients in the evaluation of brain tumors. Eur J Radiol 2005;55(03):393–400
19 Server A, Graff BA, Josefsen R, et al. Analysis of diffusion tensor imaging metrics for gliomas grading at 3 T. Eur J Radiol 2014;83 (03):e156–e165
20 Patronas NJ, Di Chiro G, Brooks RA, et al. Work in progress: [18F] fluorodeoxyglucose and positron emission tomography in the evaluation of radiation necrosis of the brain. Radiology 1982;144 (04):885–889
21 Di Chiro G, DeLaPaz RL, Brooks RA, et al. Glucose utilization of cerebral gliomas measured by [18F] fluorodeoxyglucose and positron emission tomography. Neurology 1982;32(12): 1323–1329
22 Munn Z, Barker TH, Moola S, et al. Methodological quality of case series studies: an introduction to the JBI critical appraisal tool. JBI Evid Synth 2020;18(10):2127–2133
23 Artzi M, Bokstein F, Blumenthal DT, et al. Differentiation between vasogenic-edema versus tumor-infiltrative area in patients with glioblastoma during bevacizumab therapy: a longitudinal MRI study. Eur J Radiol 2014;83(07):1250–1256
24 Wu H, Tong H, Du X, et al. Vascular habitat analysis based on dynamic susceptibility contrast perfusion MRI predicts IDH mutation status and prognosis in high-grade gliomas. Eur Radiol 2020;30(06):3254–3265
25 Valentini MC, Mellai M, Annovazzi L, et al. Comparison among conventional and advanced MRI, ^{18}F-FDG PET/CT, phenotype and genotype in glioblastoma. Oncotarget 2017;8(53):91636–91653
26 Artzi M, Blumenthal DT, Bokstein F, et al. Classification of tumor area using combined DCE and DSC MRI in patients with glioblastoma. J Neurooncol 2015;121(02):349–357
27 Oh J, Cha S, Aiken AH, et al. Quantitative apparent diffusion coefficients and T2 relaxation times in characterizing contrast enhancing brain tumors and regions of peritumoral edema. J Magn Reson Imaging 2005;21(06):701–708
28 Molina-Romero M, Wiestler B, Gomez PA, Menzel MI, Menze BH. in 21st International Conference on Medical Image Computing and Computer Assisted Intervention (MICCAI). vol. 11072. Granada, Spain: Springer International Publishing Ag;2018:98–106
29 Selker RG, Mendelow H, Walker M, Sheptak PE, Phillips JG. Pathological correlation of CT ring in recurrent, previously treated gliomas. Surg Neurol 1982;17(04):251–254
30 Kelly PJ, Daumas-Duport C, Kispert DB, Kall BA, Scheithauer BW, Illig JJ. Imaging-based stereotaxic serial biopsies in untreated intracranial glial neoplasms. J Neurosurg 1987;66 (06):865–874
31 Ramakrishna R, Barber J, Kennedy G, et al. Imaging features of invasion and preoperative and postoperative tumor burden in previously untreated glioblastoma: correlation with survival. Surg Neurol Int 2010. Doi: 10.4103/2152-7806.68337
32 Engelhorn T, Savaskan NE, Schwarz MA, et al. Cellular characterization of the peritumoral edema zone in malignant brain tumors. Cancer Sci 2009;100(10):1856–1862
33 Law M, Cha S, Knopp EA, Johnson G, Arnett J, Litt AW. High-grade gliomas and solitary metastases: differentiation by using perfusion and proton spectroscopic MR imaging. Radiology 2002;222 (03):715–721
34 Nelson SJ. Multivoxel magnetic resonance spectroscopy of brain tumors. Mol Cancer Ther 2003;2(05):497–507
35 Schiffer D, Mellai M, Annovazzi L, et al. Stem cell niches in glioblastoma: a neuropathological view. BioMed Res Int 2014; 2014:725921
36 Barajas RF Jr, Cha S. Benefits of dynamic susceptibility-weighted contrast-enhanced perfusion MRI for glioma diagnosis and therapy. CNS Oncol 2014;3(06):407–419
37 Morrice JR, Gregory-Evans CY, Shaw CA. Animal models of amyotrophic lateral sclerosis: a comparison of model validity. Neural Regen Res 2018;13(12):2050–2054
38 Maia AC Jr, Malheiros SM, da Rocha AJ, et al. MR cerebral blood volume maps correlated with vascular endothelial growth factor expression and tumor grade in nonenhancing gliomas. Am J Neuroradiol 2005;26(04):777–783
39 Cha S, Lupo JM, Chen MH, et al. Differentiation of glioblastoma multiforme and single brain metastasis by peak height and percentage of signal intensity recovery derived from dynamic susceptibility-weighted contrast-enhanced perfusion MR imaging. Am J Neuroradiol 2007;28(06):1078–1084
40 McKnight TR, von dem Bussche MH, Vigneron DB, et al. Histopathological validation of a three-dimensional magnetic resonance spectroscopy index as a predictor of tumor presence. J Neurosurg 2002;97(04):794–802
41 Croteau D, Scarpace L, Hearshen D, et al. Correlation between magnetic resonance spectroscopy imaging and image-guided biopsies: semiquantitative and qualitative histopathological analyses of patients with untreated glioma. Neurosurgery 2001;49(04):823–829
42 Pirzkall A, Li X, Oh J, et al. 3D MRSI for resected high-grade gliomas before RT: tumor extent according to metabolic activity in relation to MRI. Int J Radiat Oncol Biol Phys 2004;59(01):126–137
43 Stadlbauer A, Nimsky C, Buslei R, et al. Proton magnetic resonance spectroscopic imaging in the border zone of gliomas: correlation of metabolic and histological changes at low tumor infiltration–initial results. Invest Radiol 2007;42(04):218–223
44 Molina-Romero M, Wiestler B, Gómez PA, Menzel MI, Menze BH. in Medical Image Computing and Computer Assisted Intervention – MICCAI 2018,. Frangi AF, Schnabel JA, Davatzikos C, Alberola-López C, Fichtinger G, eds. Springer International Publishing. 2018:98–106
45 Piyapittayanan S, Chawalparit O, Tritakarn SO, et al. Value of diffusion tensor imaging in differentiating high-grade from low-grade gliomas. J Med Assoc Thai 2013;96(06):716–721
46 Alexiou GA, Zikou A, Tsiouris S, et al. Correlation of diffusion tensor, dynamic susceptibility contrast MRI and (99m)Tc-Tetrofosmin brain SPECT with tumour grade and Ki-67 immunohistochemistry in glioma. Clin Neurol Neurosurg 2014; 116:41–45
47 Price SJ, Gillard JH. Imaging biomarkers of brain tumour margin and tumour invasion. Br J Radiol 2011;84(Spec No 2):S159–S167
48 Pauleit D, Langen KJ, Floeth F, et al. Can the apparent diffusion coefficient be used as a noninvasive parameter to distinguish tumor tissue from peritumoral tissue in cerebral gliomas? J Magn Reson Imaging 2004;20(05):758–764
49 Price SJ, Jena R, Burnet NG, Carpenter TA, Pickard JD, Gillard JH. Predicting patterns of glioma recurrence using diffusion tensor imaging. Eur Radiol 2007;17(07):1675–1684
50 Yin Y, Tong D, Liu XY, et al. Correlation of apparent diffusion coefficient with Ki-67 in the diagnosis of gliomas. Zhongguo Yi Xue Ke Xue Yuan Xue Bao 2012;34(05):503–508
51 Zikou AK, Alexiou GA, Kosta P, et al. Diffusion tensor and dynamic susceptibility contrast MRI in glioblastoma. Clin Neurol Neurosurg 2012;114(06):607–612
52 Kalpathy-Cramer J, Gerstner ER, Emblem KE, Andronesi O, Rosen B. Advanced magnetic resonance imaging of the physical processes in human glioblastoma. Cancer Res 2014;74(17):4622–4637

53 Rakheja R, Chandarana H, DeMello L, et al. Correlation between standardized uptake value and apparent diffusion coefficient of neoplastic lesions evaluated with whole-body simultaneous hybrid PET/MRI. Am J Roentgenol 2013;201(05):1115–1119
54 Law M, Young R, Babb J, et al. Comparing perfusion metrics obtained from a single compartment versus pharmacokinetic modeling methods using dynamic susceptibility contrast-enhanced perfusion MR imaging with glioma grade. Am J Neuroradiol 2006;27(09):1975–1982
55 Cha S. Update on brain tumor imaging: from anatomy to physiology. Am J Neuroradiol 2006;27(03):475–487
56 Neska-Matuszewska M, Bladowska J, Sąsiadek M, Zimny A. Differentiation of glioblastoma multiforme, metastases and primary central nervous system lymphomas using multiparametric perfusion and diffusion MR imaging of a tumor core and a peritumoral zone-Searching for a practical approach. PLoS One 2018;13(01):e0191341

